Ratiometric Analyses at critical Temperatures can magnify the signal intensity of FRET-based sugar Sensors with periplasmic binding proteins

Jongsik Gam, Jae-Seok Ha, Haseong Kim, Dae-Hee Lee, Jeeyeon Lee, Seung-Goo Lee

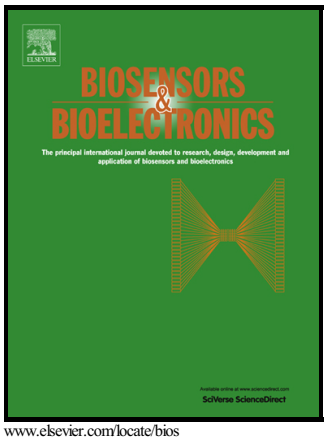

www.elsevier.com/locate/bios

PII: S0956-5663(15)30084-1
DOI: http://dx.doi.org/10.1016/j.bios.2015.04.083
Reference: BIOS7651

To appear in: *Biosensors and Bioelectronic*

Received date: 13 February 2015
Revised date: 24 April 2015
Accepted date: 25 April 2015

Cite this article as: Jongsik Gam, Jae-Seok Ha, Haseong Kim, Dae-Hee Lee, Jeeyeon Lee and Seung-Goo Lee, Ratiometric Analyses at critical Temperatures can magnify the signal intensity of FRET-based sugar Sensors with periplasmic binding proteins, *Biosensors and Bioelectronic,* http://dx.doi.org/10.1016/j.bios.2015.04.083

Ratiometric Analyses at Critical Temperatures Can Magnify the Signal Intensity of FRET-Based Sugar Sensors with Periplasmic Binding Proteins

Jongsik Gam[a,b,1], Jae-Seok Ha[a,1,§], Haseong Kim[a], Dae-Hee Lee[a,c], Jeeyeon Lee[d], and Seung-Goo Lee[a,c,*]

[a]Synthetic Biology and Bioengineering Research Center, Korea Research Institute of Bioscience and Biotechnology (KRIBB), Daejeon 305-806, Korea

[b]College of Interdisciplinary & Creative Studies, Konyang University, Nonsan-si 320-711, Korea

[c]Biosystems and Bioengineering Program, University of Science and Technology (UST), Daejeon 305-350, Korea

[d]College of Pharmacy, Seoul National University, Seoul 151-742, Korea

[*]Corresponding author: Seung-Goo Lee, Ph.D.

Mailing address: Synthetic Biology and Bioengineering Research Center, Korea Research Institute of Bioscience and Biotechnology (KRIBB), 125 Gwahak-ro, Yuseong-gu, Daejeon 305-806, Korea

E-mail address: sglee@kribb.re.kr; Phone: +82-42-860-4373; Fax: +82-42-860-4379

[§]Present address: Humedix, Co. Ltd, Anyang-si 431-809, Korea

[1]Equal contributing authors

Abstract

Fluorescence resonance energy transfer (FRET)-based sensors transduce ligand recognition into a change in the fluorophore spectrum, as ligand binding alters the distance between and orientation of two fluorescent proteins. Here, we report a dramatic increase in the signal intensity of FRET-based sugar sensors with bacterial periplasmic binding proteins (PBPs) in the binding moiety, by increasing the analysis temperature, usually higher than 50°C. The increased signal intensity results from a sudden decrease in background signal at critical temperatures, while recovering the maximum FRET ratios in the presence of ligands. When tested with a maltose sensor using a maltose-binding protein as the binding moiety, the FRET ratio at the critical temperature, 55°C, was 17-fold higher than at ambient temperatures. Similar effects were observed using analogous sensors for allose, arabinose, and glucose, providing highly dynamic and quantitative ratio changes at the critical temperatures. The proposed mechanism underlying the signal improvement is thermal relaxation of the binding proteins at the critical temperature; this hypothesis was supported by the results of intrinsic tryptophan fluorescence and circular dichroism experiments. In summary, this study shows that the conformational relaxation of proteins under specific conditions can be leveraged for highly sensitive and rapid measurements of ligands using FRET-based sensors.

Keywords: Molecular biosensor; fluorescence resonance energy transfer; critical temperature; conformation relaxation

Introduction

Protein populations in solution are a dynamic ensemble of multiple constituents with reversible conformations (Elber and Karplus 1987), in which each conformer displays different levels of functionality and stability. The reversible conformational changes of particular binding proteins have been used to develop fluorescence resonance energy transfer (FRET)-based sensors for analyzing small molecules such as calcium ions (Nagai et al. 2004), amino acids (Kaper et al. 2007; Mohsin et al. 2013; Okumoto et al. 2005), and various sugars (Ha et al. 2012). FRET-based sensors consist of donor–acceptor pairs of cyan and yellow fluorescence proteins (CFP and YFP) fused to each N- and C-terminus of the reversible binding proteins.

Under extreme conditions, some of the reversible protein conformers may contain locally unfolded structures, which are more probable near exposed surfaces or voids such as the ligand-binding site, while most other parts of the protein remain in the native state (Hoang et al. 2003; Ohmae et al. 1996). The population of locally unfolded structures can be increased under extreme conditions such as elevated temperature, low pH, or the presence of chemical denaturants (Bollen et al. 2006; Latypov et al. 2006). The locally unfolded structures can be stabilized by binding with their own ligands, resulting in a shift of the protein population to an ordered conformational state that is usually resistant to environmental stresses (Layton and Hellinga 2010; Piszczek et al. 2004). For example, a circularly permuted form of maltose-binding protein (MBP) fused with TEM1 β-lactamase protein showed increased stability in the presence of maltose (Heins et al. 2011). Consistent with this result, a destabilized mutant of dihydrofolate reductase showed restoration of a native-like structure and enhanced stability after binding its own ligand (Smith and Matthews 2001).

In current biotechnology research, the development of molecular biosensors is gaining

importance, for supplying new probes for *in vivo* imaging (Chaudhuri et al. 2011), nano-applicable sensors (Dumbrepatil et al. 2010), and highly sensitive molecular diagnosis. Various bacterial periplasmic binding proteins (PBPs) have been tested for use as reversible binding moieties in FRET-based sensors to detect maltose (Fehr et al. 2002; Gilardi et al. 1994), glucose (Deuschle et al. 2005), and ribose (Lager et al. 2003). PBPs consist of a single polypeptide chain folded into two domains, connected by a hinge region that constitutes a cleft for ligand binding (Sack et al. 1989; Spurlino et al. 1991). However, the signal intensities of FRET-based sensors have been very limited, with a Δratio ≤ 0.2 in many cases (Fehr et al. 2002; Mohsin et al. 2013). Various rational and evolutionary protein-engineering techniques have been employed to overcome this drawback. For example, optimization of the peptide linkers between the fluorescent proteins and PBPs was attempted, to improve the Δratio up to near 0.6 (Deuschle et al. 2005; Ha et al. 2007; Takanaga et al. 2008). This effort aimed to improve transfer of the motion of PBPs to the fluorescence proteins by producing tightly coupled structural combinations; however, in the absence of ligands, this combination would also produce higher background intensity.

In this study, we report that increasing assay temperatures to critical levels is highly effective for reducing background signal while retaining sensor response. That is, background signal (without a ligand) increased as the temperature increased, but then decreased to a minimal level when the critical temperature was reached. The partially unfolded conformers restored the maximum FRET ratios upon ligand binding at the determined critical temperature, resulting in increased signal-to-background ratio.

Material and methods

Preparation of biosensors

The *MBP* gene from *Escherichia coli* JM109 was cloned between the *Bam*HI and *Hin*dIII sites of the pET21a(+) vector (Novagen) to yield pET21a-MBP-6xHis. The plasmids used for expression of biosensors, containing the genes for CFP-SBP-YFP-6xHis, have been previously described (Ha et al. 2012; Ha et al. 2007). In this study, sugar binding protein (*SBP*) genes encoding allose-binding protein, arabinose-binding protein, glucose/galactose-binding protein, or MBP were used. The constructed plasmids were transformed into *E. coli* JM109(DE3) (Promega).

Biosensor proteins containing a C-terminal 6xHis-tag from the resulting constructs were expressed for 24 h at 28°C after induction with 0.5 mM isopropyl β-D-1-thiogalactopyranoside. The harvested cells were then suspended in 6xHis-tag-binding buffer (20 mM Tris-HCl, pH 8.0, 1 mM PMSF, 0.5 mM EDTA, and 1 mM DTT) and disrupted by sonication to release the CFP-SBP-YFP-6xHis proteins. The cell lysate was centrifuged for 30 min at 12,000 × *g* to remove cell debris, and the supernatant was loaded onto a Ni-NTA column (GE-Healthcare) according to the manufacturer's protocol. The purified protein biosensors were eluted and then desalted with phosphate-buffered saline (PBS, pH 7.4) containing 20% glycerol, concentrated, and stored at −70°C. Free MBP with a C-terminal 6xHis-tag was purified following the same procedure, using the pET21a-MBP-6xHis vector.

Fluorescence measurement

Fluorescence measurements were performed with 0.5 μM of purified proteins, which is an appropriate concentration to yield reproducible results with low error readouts, in PBS (pH 7.4) using a Cary Eclipse fluorescence spectrophotometer (Varian Inc., Mulgrave, Australia),

as previously described (Ha et al. 2012; Ha et al. 2007). Biosensor proteins were excited at 436 nm, and the emission intensities of CFP and YFP were measured at 480 and 530 nm, respectively. The FRET ratio was calculated by dividing the emission intensity at 530 nm by the emission intensity at 480 nm. The ΔFRET ratio indicates the FRET ratio change of biosensors with or without ligands. All experiments were repeated at least three times independently.

To investigate tryptophan fluorescence, emission spectra between 290 nm and 400 nm were measured when the protein was excited at 288 nm in PBS (pH 7.4), and then the emission intensities at 353 nm were compared in the presence or absence of maltose to analyze the effects of MBP on tryptophan fluorescence.

Characterization of temperature-dependent FRET changes

The temperature dependence of the FRET ratio of the biosensors was analyzed using a fluorescence spectrophotometer equipped with a Peltier device for temperature control. Sensor protein solutions (0.5 mL of 0.5 μM) in PBS (pH 7.4) were placed in a quartz cuvette with a stopper, and the temperature was increased from 10°C to 45°C at 5°C increments, and thereafter by 1°C increments up to 60°C. The change in FRET ratio was monitored in the absence and presence of 1 mM ligand, and the temperature showing the maximum difference was defined as the critical temperature (CT) for magnification of the signal of each biosensor.

Ligand titration experiments were performed by adding the respective sugars to proteins that had been pre-warmed to different temperatures. The ratio changes at sugar concentrations between 1 nM and 10 mM were fitted using a four-parameter Hill equation using the SigmaPlot 10.0 software (Systat Software Inc., Richmond, CA, USA), and the points corresponding to 50% saturation were determined, as the apparent dissociation constants (K_d).

Circular dichroism measurements

The effects of temperature on the secondary structures of FRET-based biosensors were investigated using a JASCO J-815 circular dichroism (CD) spectrometer (JASCO Inc., MD). Sensor protein solutions (0.5 mL of 2.2 μM) in PBS (pH 7.4) were placed in a temperature-controlled quartz cuvette of a 0.1-cm path length, and the CD spectra in the near-UV range were collected at temperatures between 25°C and 70°C. The temperature providing the maximum difference in near-UV ellipticity was determined in the absence and presence of 1 mM ligand. Then, to show the reversibility of near-UV ellipticity changes, the ellipticity data were monitored at 222 nm in the presence and absence of 1 mM maltose while the assay temperature was increased and decreased three times between 40°C and 70°C at a rate of 1°C per minute.

Results

Effect of temperature on tryptophan fluorescence of MBP

The aromatic residues of MBP, including tryptophan, tyrosine, and phenylalanine, are normally buried in nonpolar and hydrophobic environments, and the emission fluorescence at 353 nm is correlated with the water accessibility and the degree of packing of tryptophan residues in the protein structures. MBP, a PBP, displays a hinge-bending motion on maltose binding (Sharff et al. 1992), as illustrated in Fig. 1A. The protein also contains important tryptophan residues, such as W62, W230, W232, and W340, near the flexible structures involved in hinge-bending (Fig. 1C). When the tryptophan fluorescence of MBP was analyzed at various temperatures between 5°C and 65°C, it was found to decrease gradually as the temperature rose, and to drop sharply at 55°C (Fig. 1B), possibly reflecting structural

changes near the tryptophan residues. However, when the tryptophan fluorescence of MBP was analyzed in the presence of 10 mM maltose, the fluorescence intensity remained more stable at the same temperatures (Fig. 1B), indicating that the structural moiety was stabilized by binding with maltose. This shift in tryptophan fluorescence is consistent with previous findings that the thermal melting of MBP is retarded by ligand binding (Layton and Hellinga 2010; Piszczek et al. 2004). At temperatures over 65°C, tryptophan fluorescence was not altered by maltose binding, implying that the protein had lost its binding capability (Figure 1B).

Signal magnification of FRET-based biosensors at elevated temperatures

The specific responses of MBP at elevated temperatures were also examined using two FRET-based biosensors, CMY-0 and CMY-BII, with different dipeptide linkers (Ha et al. 2007) (Fig. 1D). First, when the CMY-0 sensor was tested, with no additional linker between MBP and YFP, strong drift of the ratio profiles was observed at 55°C (Fig. 1E), very similar to the aforementioned drift in tryptophan fluorescence, shown in Fig. 1B. The change in ratio observed with maltose was calculated to be approximately 0.85, which is 17-fold higher than at 25°C. At 65°C, the ratio change was no longer observed. Similar results were observed using another maltose biosensor, CMY-BII, with an optimized dipeptide linker (Ha et al. 2007). The temperature profiles of CMY-BII differed slightly from those of CMY-0; this difference might have been caused by the concomitant temperature-dependent change in the linker moiety in CMY-BII. Here, a 7.2-fold increase in FRET ratio was observed at 55°C (Fig. 1F). Magnification of the signal of the FRET-based sensors using critical temperature was tested with other biosensors, using allose-, arabinose-, and glucose-binding proteins in the receptor moiety. The CT was found to be 50°C for all, yielding apparent ratio changes of -0.63, 0.72, and 1.58 in the presence of allose, arabinose and glucose, respectively

(Supplementary Fig. 1A, 1B, and 1C). The signal was observed to be magnified by 3.0-, 2.5-, and 12.1-fold in the presence of allose, arabinose, and glucose, respectively, compared to the respective signals at 25°C (Table 1).

Next, free MBP without fusion of fluorescent proteins was titrated with maltose at different temperatures, and the intrinsic tryptophan fluorescence was monitored. At 55°C, the change in tryptophan fluorescence for MBP exhibited a sigmoid response curve as the maltose concentration increased, whereas at 25°C, it exhibited a relatively small change. The K_d with maltose was estimated to be 7.1 μM at 55°C (Supplementary Fig. 2) and 1.0 μM at 25°C, similar to the previously reported value of 0.63 μM (Rizk et al. 2011). Likewise, the ratio change for a FRET-based biosensor, CMY-BII, indicated a larger response at 55°C than at 25°C upon titration of maltose (Fig. 2A). The apparent K_d value was 25.6 μM at 55°C and 1.8 μM at 25°C (Table 1). Ligand titration was also performed for the three sugar sensors. The allose sensor (Fig. 2B) produced a negative sigmoid curve, whereas the arabinose sensor produced a typical sigmoid curve (Fig. 2C). The K_d values for allose and arabinose were 8.4 μM and 67 μM, respectively, at 50°C; these were 23-fold and 186-fold higher than the K_d values at 25°C (Table 1). Interestingly, the glucose sensor showed a negative sigmoid curve at 25°C, but produced an opposite sigmoid curve at 50°C (Fig. 2D). The K_d for the glucose sensor was 9.2 μM at 50°C, which was 12.1 times higher than at 25°C.

Ligand specificity at elevated temperatures

To evaluate the ligand specificity at elevated temperatures, the FRET ratios of the four biosensors were measured in the presence of 18 available sugars, including mono-, di-, and oligosaccharides, and sugar alcohols, using 0, 0.1, 1, and 10 mM of each sugar. At the

elevated temperatures, the maltose sensor (CMY-BII) and the allose sensor responded to their ligands with high specificity (Fig. 3A and 3B), as at 25°C (solid lines in Fig. 3). The arabinose sensor showed a higher specificity at the elevated temperature, becoming insensitive to D-xylose and D-lactose (Fig. 3C). The glucose sensor showed slightly improved specificity at the elevated temperature, but still exhibited broad binding affinities toward various sugars, as it did at 25°C (Fig. 3D). The improved specificity of the arabinose and the glucose biosensors, the latter of which is a relatively promiscuous sensor, is likely to be the consequence of decreased affinity of the biosensors to non-canonical ligands at elevated temperatures.

Circular dichroism analyses of thermal effects on FRET biosensors

Near-UV CD spectra of CMY-BII were investigated at temperatures between 25°C and 70°C in the absence and presence of 1 mM maltose. As shown in Fig. 4A, at 55°C and 222 nm (shown as a double-headed arrow in Fig. 4A), the CD spectra differed markedly in the presence or absence of maltose, whereas those at 45°C and 65°C were almost identical. The large difference, particularly near 222 nm, may indicate that more α-helixes unfolded into unordered structures at this temperature in the absence of the ligand (Greenfield 2006). Next, the temperature was cycled between 40°C and 70°C three times, and the ellipticity was monitored at 222 nm, as shown in Fig. 4B. The full recurrence of the ellipticity changes at 222 nm implies that the unfolding of the α-helix is completely reversible. The mid-point of reversible unfolding was calculated to be 53°C in the absence of maltose; this shifted to 60°C in the presence of 1 mM maltose. These results are concordant with the hypothesis that the reversible unfolding occurs within the MBP moiety, because the fluorescent protein primarily consists of β-sheets and maintains high stability up to 70°C (Vessoni Penna et al. 2004).

Discussion

Increasing the ratio change upon ligand binding is an important issue in the field of FRET-based sensors, as this is a key factor in signal sensitivity or detectability over background noise (Ha et al. 2007; Lager et al. 2006). The change in FRET levels in the maltose sensor is actuated by the structural flip-flop motion of receptor proteins; this motion is transferred to the donor and acceptor fluorescent proteins and alters the distance between and orientation of the fluorescent proteins. In this study, FRET-based maltose sensors patterned on the *E. coli* MBP displayed a sudden drop in background FRET at 55°C, but recovered ordinary FRET levels in the presence of maltose, resulting in very large FRET ratio differences that depended on the maltose concentration. Furthermore, three other FRET-based biosensors based on the *E. coli* allose-binding, arabinose-binding, and glucose/galactose-binding proteins also displayed clear ratio magnification at 50°C. Each FRET sensor presented in this study had its own specific CT for signal intensification. Thus, different sugar sensors may have different CTs. The larger K_d values observed at critical temperatures might also be beneficial for direct detection of ligands in biological samples.

CD analysis of CMY-BII was performed to understand the conformational changes that occur at elevated temperatures. The CD spectrum of the sensor exhibited remarkable maltose-dependent changes at 55°C, but no changes were observed at 45°C (Fig. 4B). The ellipticity change observed at 222 nm was concordant with the tryptophan fluorescence profiles shown in Fig. 1C and with the FRET changes shown in Fig. 2B and 2C, suggesting that conformational changes to the secondary structure could be caused by the α-helix structure in the receptor moiety. In similar contexts, the lower background FRETs of allose, arabinose, and glucose sensors could be caused by new conformations with partially or locally unfolded moieties that exist mainly at elevated temperatures, as their behavior in the presence of their

respective ligands is similar to that of the maltose sensors in the presence of maltose.

Elevated temperature generally induces a metastable state in the sensor protein, causing conformational changes around the ligand-binding pockets of proteins, accompanied by a decrease in ligand binding affinity. The α-helix region (residues 229–239) in the cleft of the ligand-binding site and the hinge region between the N- and C-subdomains of MBP have been shown to be unstable moieties in crystallographic studies (Mueller et al. 2000). NMR structure studies have also reported the α-helix region of MBP to have high flexibility (Gardner et al. 1998; Mueller et al. 2000), whereas contact with its ligand was shown to stabilize the α-helix structure, in a crystallography study (Sharff et al. 1993). Therefore, these regions are believed to be susceptible to thermal melting and to form a relaxed conformation at elevated temperatures. The protein also contains important tryptophan residues, such as W62, W230, W232, and W340, near the flexible structures for bending of the hinge (Fig. 1C). The thermal effect, which determines whether the α-helix is relaxed or ordered, seems likely to leverage the hinge-bending motion of the various PBPs tested in this study, resulting in remarkable changes in FRET levels. In addition, it should be mentioned that pre-warming of the sugars to their respective CTs produced no significant differences in sensor signals, although the sugars might show conformational changes at elevated temperatures. This result indicates that sugar conformations rapidly equilibrate to a given temperature, more rapidly than ligand binding to the sensor protein, and thus do not affect the observations made using the sensor proteins.

Here we propose a schematic model of the effect of the critical temperature on the FRET ratio changes (Scheme 1). The flexible α-helix and hinge regions of the ligand-bound species iii should be well ordered and show a compact conformation, yielding a high FRET level. The partial melting of the α-helix in the ligand-free species ii is thought to show a loose

conformation, yielding a low FRET level, but the α-helix in the ligand-free species i at ambient temperature, 25°C, may retain a relatively compact conformation, even in the absence of the ligand. Eventually, the differences in FRET effect between species ii and iii at the critical temperature, 55°C, are much greater than those between species i and iii at the ambient temperature, 25°C. The presence of species ii, which shows a different state from species i and iii, will reduce the FRET background signal from ligand-unbound species i when the critical temperature is reached.

Conclusion

We revealed a new detection mode to increase the signal intensity and simultaneously to expand the dynamic range of FRET-based sugar sensors by detecting FRET ratio differences between a relaxed conformer and an ordered conformer at critical temperatures that partially melt the secondary structure at the ligand-binding site. The presence of ligands at the critical temperature increased the ligand-dependent FRET changes by 3–17-fold, simply by adjusting the analysis temperatures. The detection mode presented in this study has practical significance for *in vitro* analyses of sugars; the temperature can be altered repeatedly to control the sensor signal with no chemical changes during analysis. The readouts can easily be monitored in the laboratory using a common fluorometer or inexpensive LED equipment. Moreover, this detection mode could be useful for high-throughput analysis using limited quantities of sensor proteins, such as biosensors immobilized on bead surfaces or on the bottom of micro-well plates.

Acknowledgements

This research was supported by grants from the Intelligent Synthetic Biology Center of

Global Frontier Project (2011-0031944), the Next-Generation Biogreen 21 Program (PJ009524), the Bio-industry Technology Development Program (No. 310006-5), and the KRIBB Research Initiative Program.

References

Bollen, Y.J., Kamphuis, M.B., van Mierlo, C.P., 2006. The folding energy landscape of apoflavodoxin is rugged: hydrogen exchange reveals nonproductive misfolded intermediates. Proc Natl Acad Sci U S A 103(11), 4095-4100.

Chaudhuri, B., Hormann, F., Frommer, W.B., 2011. Dynamic imaging of glucose flux impedance using FRET sensors in wild-type Arabidopsis plants. Journal of experimental botany 62(7), 2411-2417.

Deuschle, K., Okumoto, S., Fehr, M., Looger, L.L., Kozhukh, L., Frommer, W.B., 2005. Construction and optimization of a family of genetically encoded metabolite sensors by semirational protein engineering. Protein Sci 14(9), 2304-2314.

Dumbrepatil, A.B., Lee, S.G., Chung, S.J., Lee, M.G., Park, B.C., Kim, T.J., Woo, E.J., 2010. Development of a nanoparticle-based FRET sensor for ultrasensitive detection of phytoestrogen compounds. The Analyst 135(11), 2879-2886.

Elber, R., Karplus, M., 1987. Multiple conformational states of proteins: a molecular dynamics analysis of myoglobin. Science (New York, N.Y.) 235(4786), 318-321.

Fehr, M., Frommer, W.B., Lalonde, S., 2002. Visualization of maltose uptake in living yeast cells by fluorescent nanosensors. Proc Natl Acad Sci U S A 99(15), 9846-9851.

Gardner, K.H., Zhang, X., Gehring, K., Kay, L.E., 1998. Solution NMR Studies of a 42 KDa Escherichia Coli Maltose Binding Protein/β-Cyclodextrin Complex: Chemical Shift Assignments and Analysis. J. Am. Chem. Soc. 120 (45), 11738–11748.

Gilardi, G., Zhou, L.Q., Hibbert, L., Cass, A.E., 1994. Engineering the maltose binding protein for reagentless fluorescence sensing. Anal Chem 66(21), 3840-3847.

Greenfield, N.J., 2006. Analysis of the kinetics of folding of proteins and peptides using circular dichroism. Nature protocols 1(6), 2891-2899.

Ha, J.S., Gam, J., Choi, S.L., Oh, K.H., Ro, H.S., Song, J.J., Shin, C.S., Lee, S.G., 2012. Quantitative analyses of individual sugars in mixture using FRET-based biosensors. Biotechnology progress 28(5), 1376-1383.

Ha, J.S., Song, J.J., Lee, Y.M., Kim, S.J., Sohn, J.H., Shin, C.S., Lee, S.G., 2007. Design and application of highly responsive fluorescence resonance energy transfer biosensors for detection of sugar in living Saccharomyces cerevisiae cells. Appl Environ Microbiol 73(22), 7408-7414.

Heins, R.A., Choi, J.H., Sohka, T., Ostermeier, M., 2011. In vitro recombination of non-homologous genes can result in gene fusions that confer a switching phenotype to cells. PloS one 6(11), e27302.

Hoang, L., Maity, H., Krishna, M.M., Lin, Y., Englander, S.W., 2003. Folding units govern the cytochrome c alkaline transition. J Mol Biol 331(1), 37-43.

Kaper, T., Looger, L.L., Takanaga, H., Platten, M., Steinman, L., Frommer, W.B., 2007. Nanosensor detection of an immunoregulatory tryptophan influx/kynurenine efflux cycle. PLoS biology 5(10), e257.

Lager, I., Fehr, M., Frommer, W.B., Lalonde, S., 2003. Development of a fluorescent nanosensor for ribose. FEBS Letters 553(1-2), 85-89.

Lager, I., Looger, L.L., Hilpert, M., Lalonde, S., Frommer, W.B., 2006. Conversion of a putative Agrobacterium sugar-binding protein into a FRET sensor with high selectivity for sucrose. J Biol Chem 281(41), 30875-30883.

Latypov, R.F., Cheng, H., Roder, N.A., Zhang, J., Roder, H., 2006. Structural characterization

of an equilibrium unfolding intermediate in cytochrome c. J Mol Biol 357(3), 1009-1025.

Layton, C.J., Hellinga, H.W., 2010. Thermodynamic analysis of ligand-induced changes in protein thermal unfolding applied to high-throughput determination of ligand affinities with extrinsic fluorescent dyes. Biochemistry 49(51), 10831-10841.

Mohsin, M., Abdin, M.Z., Nischal, L., Kardam, H., Ahmad, A., 2013. Genetically encoded FRET-based nanosensor for in vivo measurement of leucine. Biosensors & bioelectronics 50, 72-77.

Mueller, G.A., Choy, W.Y., Yang, D., Forman-Kay, J.D., Venters, R.A., Kay, L.E., 2000. Global folds of proteins with low densities of NOEs using residual dipolar couplings: application to the 370-residue maltodextrin-binding protein. J Mol Biol 300(1), 197-212.

Nagai, T., Yamada, S., Tominaga, T., Ichikawa, M., Miyawaki, A., 2004. Expanded dynamic range of fluorescent indicators for Ca(2+) by circularly permuted yellow fluorescent proteins. Proc Natl Acad Sci U S A 101(29), 10554-10559.

Ohmae, E., Kurumiya, T., Makino, S., Gekko, K., 1996. Acid and thermal unfolding of Escherichia coli dihydrofolate reductase. Journal of biochemistry 120(5), 946-953.

Okumoto, S., Looger, L.L., Micheva, K.D., Reimer, R.J., Smith, S.J., Frommer, W.B., 2005. Detection of glutamate release from neurons by genetically encoded surface-displayed FRET nanosensors. Proc Natl Acad Sci U S A 102(24), 8740-8745.

Piszczek, G., D'Auria, S., Staiano, M., Rossi, M., Ginsburg, A., 2004. Conformational stability and domain coupling in D-glucose/D-galactose-binding protein from Escherichia coli. The Biochemical journal 381(Pt 1), 97-103.

Rizk, S.S., Paduch, M., Heithaus, J.H., Duguid, E.M., Sandstrom, A., Kossiakoff, A.A., 2011. Allosteric control of ligand-binding affinity using engineered conformation-specific effector proteins. Nature structural & molecular biology 18(4), 437-442.

Sack, J.S., Trakhanov, S.D., Tsigannik, I.H., Quiocho, F.A., 1989. Structure of the L-leucine-

binding protein refined at 2.4 A resolution and comparison with the Leu/Ile/Val-binding protein structure. J Mol Biol 206(1), 193-207.

Sharff, A.J., Rodseth, L.E., Quiocho, F.A., 1993. Refined 1.8-A structure reveals the mode of binding of beta-cyclodextrin to the maltodextrin binding protein. Biochemistry 32(40), 10553-10559.

Sharff, A.J., Rodseth, L.E., Spurlino, J.C., Quiocho, F.A., 1992. Crystallographic evidence of a large ligand-induced hinge-twist motion between the two domains of the maltodextrin binding protein involved in active transport and chemotaxis. Biochemistry 31(44), 10657-10663.

Smith, V.F., Matthews, C.R., 2001. Testing the role of chain connectivity on the stability and structure of dihydrofolate reductase from E. coli: fragment complementation and circular permutation reveal stable, alternatively folded forms. Protein Sci 10(1), 116-128.

Spurlino, J.C., Lu, G.Y., Quiocho, F.A., 1991. The 2.3-A resolution structure of the maltose- or maltodextrin-binding protein, a primary receptor of bacterial active transport and chemotaxis. J Biol Chem 266(8), 5202-5219.

Takanaga, H., Chaudhuri, B., Frommer, W.B., 2008. GLUT1 and GLUT9 as major contributors to glucose influx in HepG2 cells identified by a high sensitivity intramolecular FRET glucose sensor. Biochimica et biophysica acta 1778(4), 1091-1099.

Vessoni Penna, T.C., Ishii, M., Cholewa, O., de Souza, L.C., 2004. Thermal characteristics of recombinant green fluorescent protein (GFPuv) extracted from Escherichia coli. Letters in applied microbiology 38(2), 135-139.

Figure legends

Figure 1. Temperature effect on ligand binding of maltose-binding protein (MBP). (A) Schematic drawing of the global conformational change of MBP upon maltose binding. (B) Structure of the MBP-maltose complex (PDB ID: 1ANF) showing tryptophan residues (green) on the binding site. (C) Temperature effect on intrinsic fluorescence intensity of MBP. Fluorescence intensity at 353 nm was measured when MBP was excited at 288 nm. (D) Schematic drawing of a FRET-based biosensor illustrating the mechanism of the change in FRET ratio upon ligand binding. Temperature effects on changes in the FRET ratio of the FRET-based maltose sensors, (E) CMY-0 (maltose sensor without a linker), (F) CMY-BII (maltose sensor with a optimized linker), in the absence (filled symbols, ●) and in the presence (empty symbols, ○) of 10 mM maltose. The FRET ratio between fluorescence emissions at 530 and 480 nm was measured when biosensors were excited at 436 nm. C and Y represent for CFP and YFP fused on N- and C-termini of MBP as a FRET pair.

Figure 2. Sugar titration curves of the change in FRET ratio for the FRET-based sensors, (A) maltose sensor (CMY-BII), (B) allose sensor, (C) arabinose sensor, and (D) glucose sensor (GGBP-SS) for detection of maltose, allose, arabinose, and glucose, respectively, measured at 25°C (filled symbols, ●) and at the critical temperatures (empty symbols, ○).

Figure 3. Comparison of the ligand specificity of fluorescence resonance energy transfer (FRET)-based sugar sensors at the critical temperature. The FRET ratios for purified (A) maltose (CMY-BII), (B) allose (ALBP-QV), (C) arabinose (ARBP-PR), and (D) glucose/galactose (GGBP-SS) sensors were determined in the presence of various mono-, di-,

and trisaccharides, and sugar alcohols at different concentrations in phosphate-buffered saline, pH 7.4. ■; 0 mM, ▨; 0.1 mM, ▧; 1 mM, □; 10 mM. The arrowhead represents the canonical sugar for the sensor. Solid line graphs with empty circles show FRET ratios measured at 25°C (from the previous paper, Ha et al. 2012).

Figure 4. Circular dichroism (CD) measurement of CMY-BII. (A) Circular dichroism spectra at 45°C (solid lines), 55°C (dashed lines), and 65°C (dash-dot lines) in the presence (black lines) and absence (grey lines) of 1 mM maltose. The double-headed arrow indicates a significant difference in ellipticity associated with the presence of maltose at critical temperature, 55°C. CD spectra at other temperatures have been omitted for clarity. (B) 3-recycles of temperature increase and decrease between 40 and 70°C in the absence of maltose (filled symbols, ●) and in the presence of 1 mM maltose (empty symbols, ○) with 1°C decrement per minute.

CT = Critical temperature for reversible signal amplification

Maximum change of 530/480 nm FRET ratio in response to sugars at critical temperature (CT) and room tem

$\Delta ratio = (I_{530}/I_{480})_{lig} - (I_{530}/I_{480})_{apo}$; I_{530} and I_{480} are emission intensities of the acceptor and the donor with liga

ligand (apo).

K_d ± standard deviation for concentration of sugars that induced half-maximal increase in the intensity ratio

Dynamic range was estimated (defined here) from 10% to 90% of minimum and maximum of signal respond

ND = not determined.

a and *b* The Δratio and K_d values at 25°C are from the previous sugar sensor papers (Ha *et al*. 2007[a] and 2012

Scheme 1. Proposed schematic model of the temperature-dependent effect on conformational relaxation of FRET-based biosensors: ordered state (i) at ambient temperature in the absence of ligand and (ii) at critical temperature in the presence of ligand to give remarkably enhanced Δratio from the relaxed conformation (iii) at critical temperature in the absence of ligand.

Highlights

- We examined the critical temperature effect on FRET-based sensors.
- The FRET ratio change of maltose sensor was dramatically increased at critical temperature.
- The temperature effect was also observed in other FRET-base sugar sensors.
- The proposed mechanism is thermal relaxation affecting ligand-binding states.

Table 1. Thermal characteristics of FRET biosensors for glucose, allose, arabinose, and maltose at optimal conditions

Sugar Sensors	CT (°C)	Δratio at CT	Δratio at 25°C	Δratio fold ($\Delta ratio^{CT}$/ $\Delta ratio^{25°C}$)	K_d (μM) at CT	K_d (μM) at 25 °C	K_d ratio (K_d^{CT}/ $K_d^{25°C}$)	Dynamic range (μM) at CT
CMY-0 for maltose	55	0.85	0.05[a]	17	ND	2.4 ± 0.2[a]	ND	ND
CMY-BII for maltose	55	1.22	0.17[a]	7.2	25.6 ± 2.0	1.8 ± 0.1[a]	14	3.1~180
ALBP-QV for allose	50	-0.63	-0.21[b]	3.0	8.4 ± 0.5	0.35 ± 0.02[b]	23	2.0~74
ARBP-PR for arabinose	50	0.72	0.29 [b]	2.5	67 ± 4.0	0.36 ± 0.01[b]	186	8.7~490
GGBP-SS for glucose	50	1.58	-0.13[b]	12.1	9.2 ± 0.5	0.18 ± 0.03[b]	50	1.5~57

CT = Critical temperature for reversible signal amplification

Maximum change of 530/480 nm FRET ratio in response to sugars at critical temperature (CT) and room temperature (25°C).

Δratio = $(I_{530}/I_{480})_{lig}$ - $(I_{530}/I_{480})_{apo}$; I_{530} and I_{480} are emission intensities of the acceptor and the donor with ligand (lig) or without ligand (apo).

K_d ± standard deviation for concentration of sugars that induced half-maximal increase in the intensity ratio of 530/480 nm.

Dynamic range was estimated (defined here) from 10% to 90% of minimum and maximum of signal responding range.

ND = not determined.

[a] and [b] The Δratio and K_d values at 25°C are from the previous sugar sensor papers (Ha *et al*. 2007[a] and 2012[b]).

Figure 1

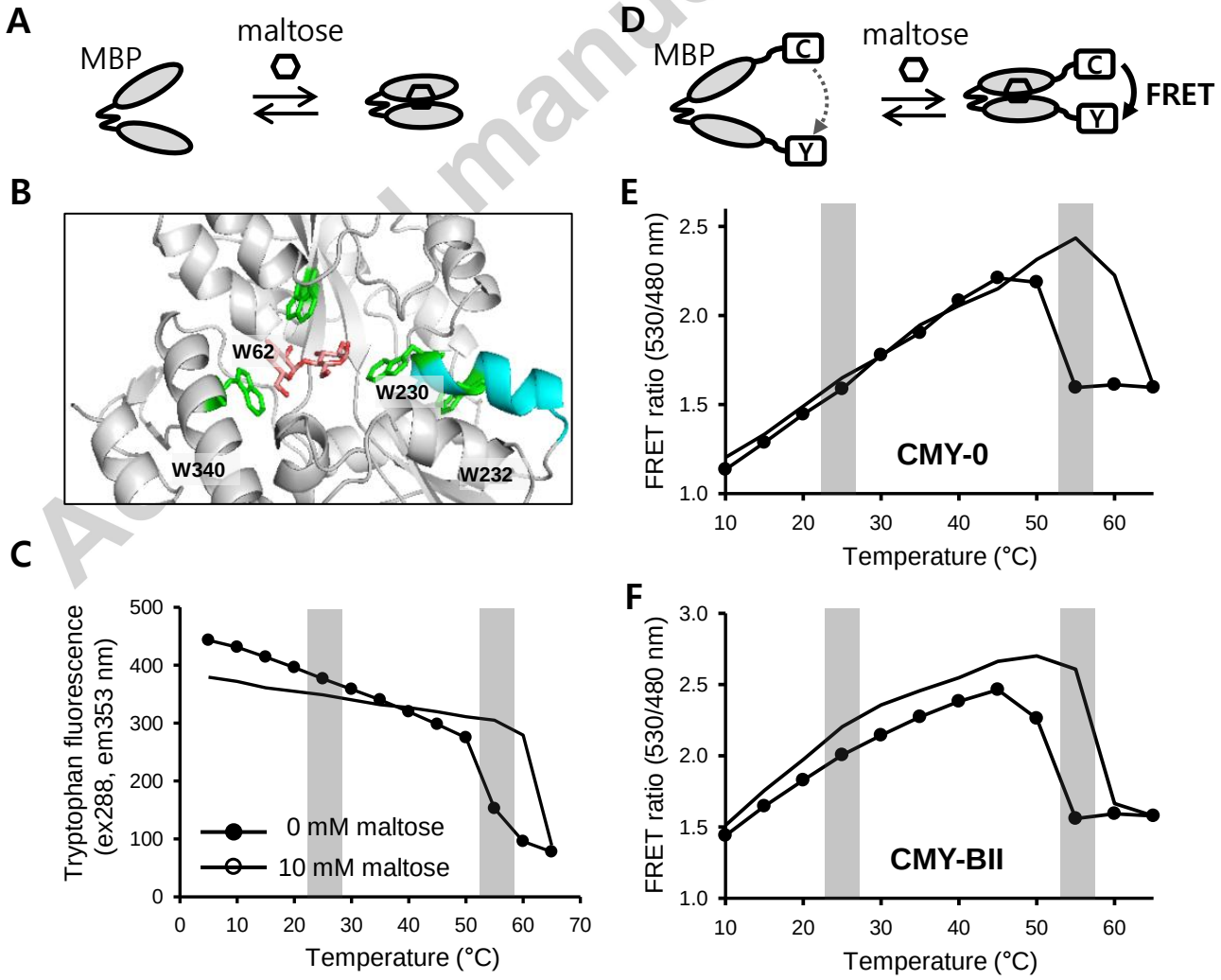

Figure 2

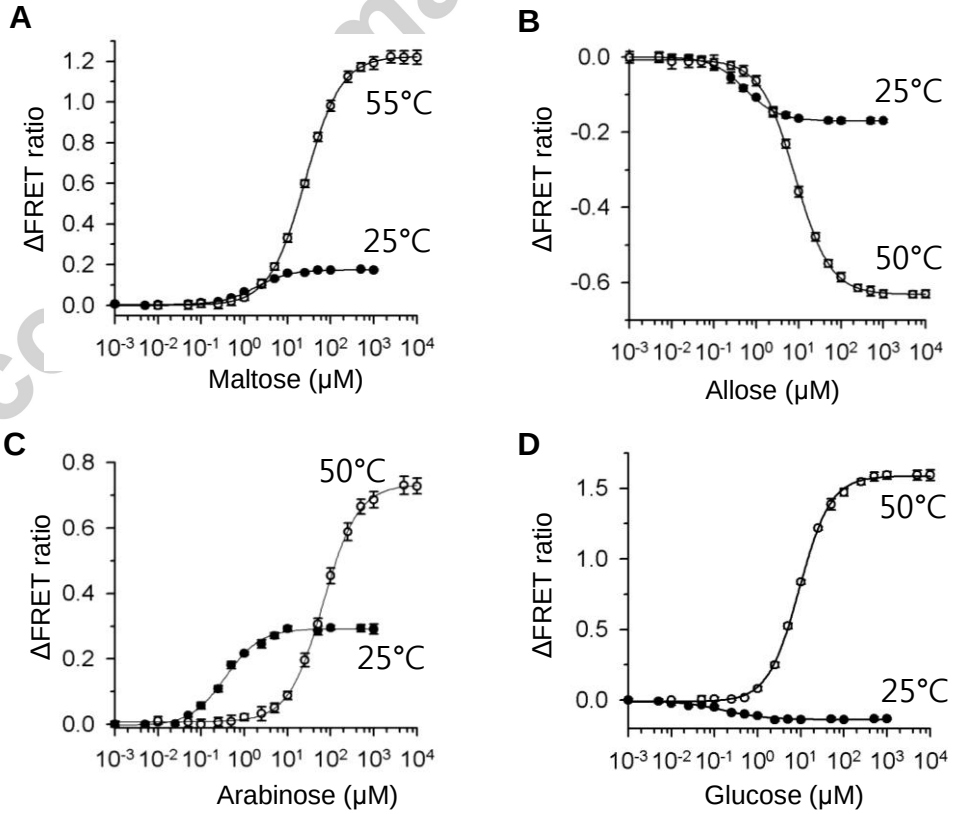

Figure 3

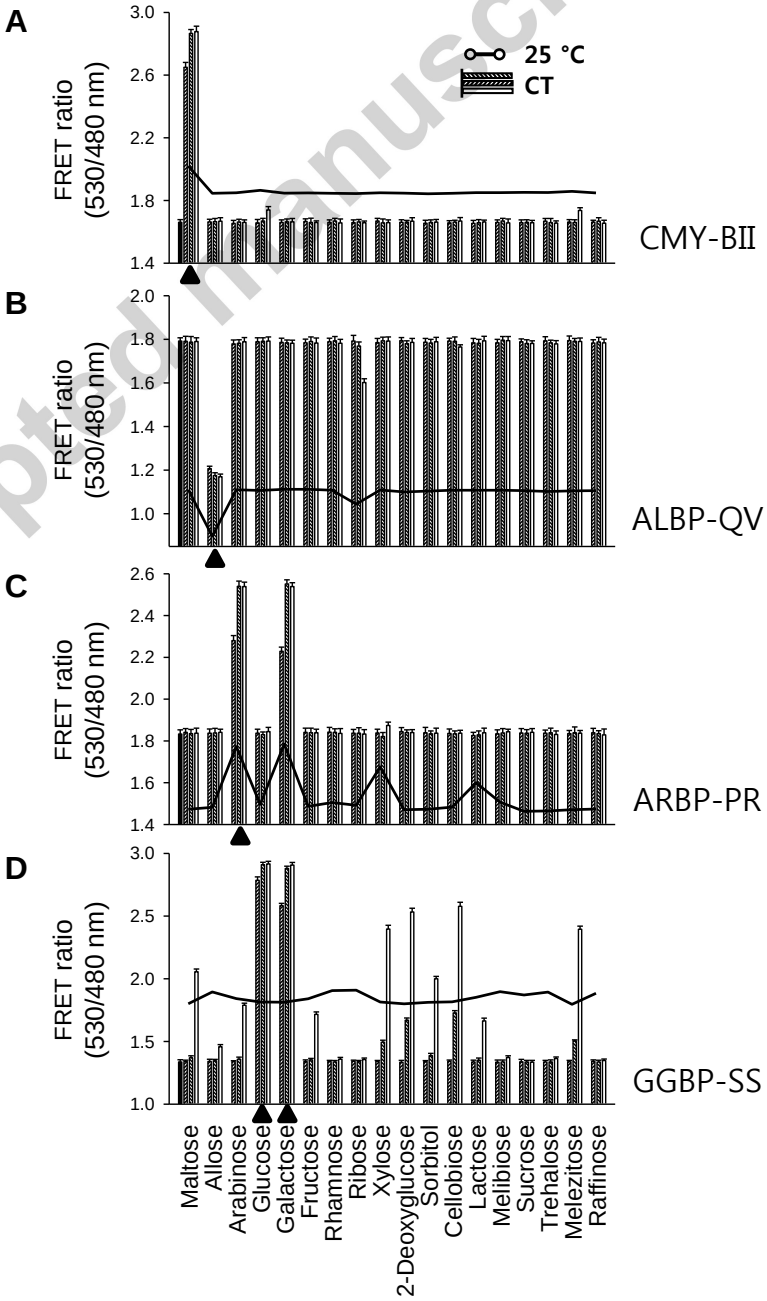

Figure 4

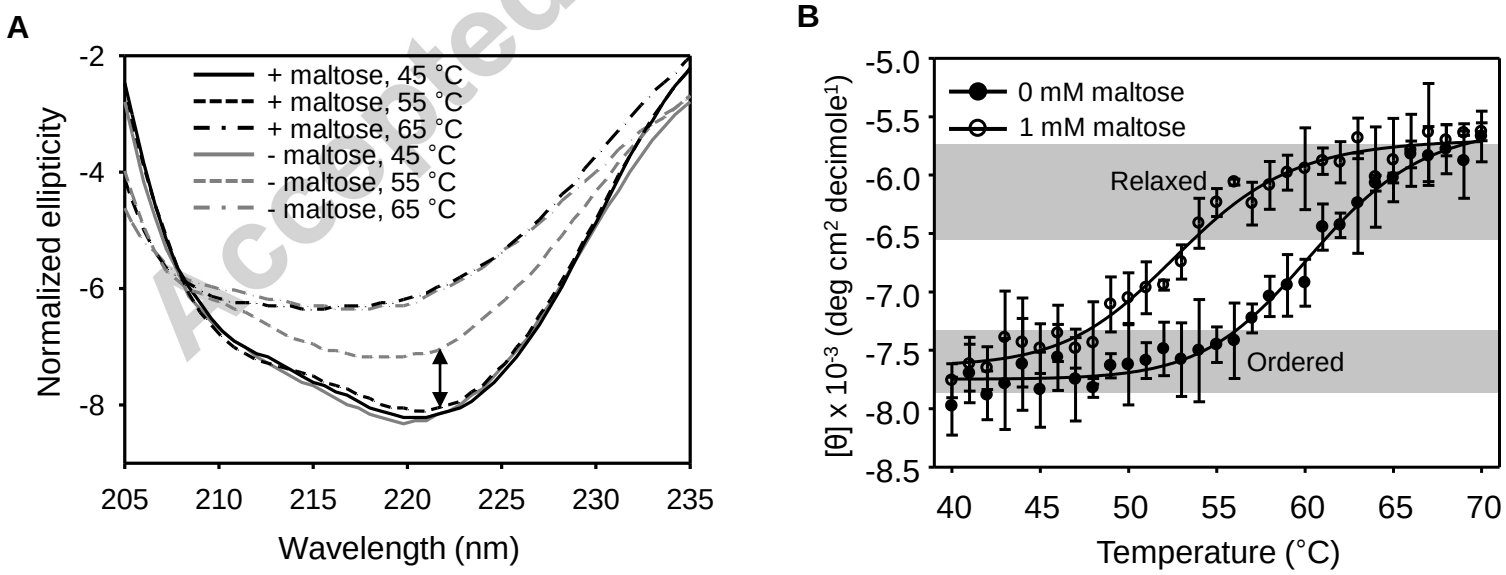

Scheme 1